

AD-A267 760



FASTC-ID(RS)T-0730-92

FOREIGN AEROSPACE SCIENCE AND TECHNOLOGY CENTER



EXPERIMENTAL STUDY ON INTERFERENCE AERODYNAMICS
OF CLOSE-COUPLED CANARD CONFIGURATION

by

Guo Yaobin

DTIC
ELECTE
AUG 11 1993
S B D



Approved for public release;
Distribution unlimited.

93-18427



1998

93 8 10 268

HUMAN TRANSLATION

FASTC-ID(RS)T-0730-92 20 July 1993

MICROFICHE NR: 93C000463

EXPERIMENTAL STUDY ON INTERFERENCE AERODYNAMICS
OF CLOSE-COUPLED CANARD CONFIGURATION

By: Guo Yaobin

English pages: 15

Source: Hangkong Xuebao, Vol. 11, Nr. 12, 1990;
pp. 528-533

Country of origin: China

Translated by: Leo Kanner Associates
F33657-88-D-2188

Requester: FASTC/TATV/Paul Freisthler

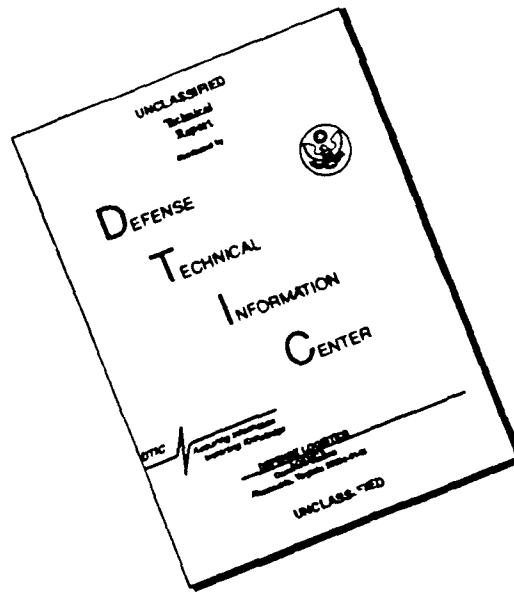
Approved for public release; Distribution unlimited.

THIS TRANSLATION IS A RENDITION OF THE ORIGINAL
FOREIGN TEXT WITHOUT ANY ANALYTICAL OR EDITO-
RIAL COMMENT STATEMENTS OR THEORIES ADVOC-
ATED OR IMPLIED ARE THOSE OF THE SOURCE AND
DO NOT NECESSARILY REFLECT THE POSITION OR
OPINION OF THE FOREIGN AEROSPACE SCIENCE AND
TECHNOLOGY CENTER.

PREPARED BY:

TRANSLATION DIVISION
FOREIGN AEROSPACE SCIENCE AND
TECHNOLOGY CENTER
WPAFB, OHIO

DISCLAIMER NOTICE



THIS DOCUMENT IS BEST QUALITY AVAILABLE. THE COPY FURNISHED TO DTIC CONTAINED A SIGNIFICANT NUMBER OF PAGES WHICH DO NOT REPRODUCE LEGIBLY.

GRAPHICS DISCLAIMER

All figures, graphics, tables, equations, etc. merged into this translation were extracted from the best quality copy available.

DTIC QUALITY INSPECTED 3

Accession For	
NTIS GRA&I	<input checked="checked" type="checkbox"/>
DTIC TAB	<input type="checkbox"/>
Unannounced	<input type="checkbox"/>
Justification	
By	
Distribution/	
Availability Codes	
Dist	Avail and/or Special
A-1	

EXPERIMENTAL STUDY ON INTERFERENCE AERODYNAMICS
OF CLOSE-COUPLED CANARD CONFIGURATION

Guo Yaobin

Harbin Aerodynamics Research Institute

Abstract: By using the canard-wing balance and the whole-aircraft aerodynamic balance, which can measure the aerodynamic forces of the canard-wing part, experimental studies were conducted on interference aerodynamic forces on a canard-configuration model that can be assembled and disassembled. It was discovered that the interferences are destructive between the canard wing and the main wing when $\alpha < 20^\circ$, causing a reduction in the lift. When $\alpha > 32^\circ$, the interferences turn increasingly beneficial. When $\alpha = 32^\circ$, the interference lift increases to 24 percent of total lift. If the main wing is a swept-forward wing, the aerodynamic properties of the canard configuration are better.

Keywords: experimental aerodynamics, aerodynamic interference, canard configuration.

I. Foreword

Present-day requirements stipulate that a fighter aircraft should have high maneuverability and be capable of flight at large angles of attack. After the powered-control technique is adopted, an aircraft can be designed for statical instability. This will further enhance aircraft maneuverability. After trimming of the canard-model aircraft, it has excellent lift and drag properties, and frequently it is statically unstable. This approach is an important layout to be selected for the future new model fighters. For a deeper understanding of the aerodynamic properties of the canard configuration, since 1980 double balances were used in measuring the aerodynamic forces; at the same time observations are being made on the wing surface and spatial flowfields. Thus, the author derived the rule of variation in interference lift and the generating regime for interference lift of a canard configuration. In the paper, all coefficients of aerodynamic forces are given as the reference area of the main wing surface.

II. Research Method

By using the method of assembling and disassembling components with double balances, the interference aerodynamic forces between the main wing and the canard wing were studied for the canard configuration. The double balances are the canard-wing balance and the whole-aircraft balance. For the canard-wing balance, measurements were made on only the aerodynamic forces of the forebody, or the combination of forebody and canard wing. In

the case of the whole-aircraft balance, measurements were made on the aerodynamic forces of the whole aircraft, or the aircraft minus the wing, or the aircraft minus the canard wing, or the fuselage only. For a combination of different components, the results of direct measurements by both balances are listed in Table 1.

After proper combinations of the above-mentioned measurement results, the required amounts of interference can be found. By using lift as an example, the following explanations are given.

From the results of the canard-wing balance, the interference lift of the main wing acting on the canard wing can be derived (W -- main wing; C -- canard wing).

$$\Delta C_{y_{wc}} = \text{Diagram 1} - \text{Diagram 2} - \text{Diagram 3} + \text{Diagram 4} \quad (1)$$





From the results of the whole-aircraft balance, the mutual interference lift between the canard wing and the main wing can be derived.

$$\Delta C_{y_{wc}} + \Delta C_{y_{cw}} = \text{Diagram 1} - \text{Diagram 2} - \text{Diagram 3} + \text{Diagram 4} \quad (2)$$

From Eqs. (1) and (2), the interference lift produced on the main wing by the canard wing can be derived.

$$\Delta C_{y_{cw}} = (2) - (1) \quad (3)$$

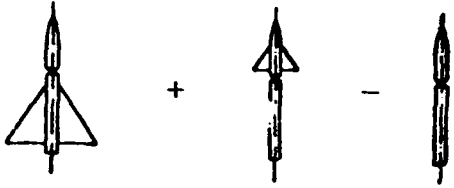
TABLE 1. MEASUREMENT RESULTS OF WHOLE-AIRCRAFT
BALANCE AND CANARD-WING BALANCE FOR DIFFERENT
MODEL STATES

1 模型状态	2 全机天平结果	3 鸭翼天平结果
	4 前机身 + 后机身 + (前机身 \rightleftharpoons 后机身)①	5 前机身 + (后机身 \rightarrow 前机身)
	6 鸭翼 + 机身 + (鸭翼 \rightleftharpoons 机身)	7 鸭翼 + 前机身 + (鸭翼 \rightleftharpoons 前机身) + (后机身 \rightarrow 前机身) + (后机身 \rightarrow 鸭翼)
	8 主翼 + 机身 + (主翼 \rightleftharpoons 机身)	9 前机身 + (后机身 \rightarrow 前机身) + (主翼 \rightarrow 前机身)
	10 鸭翼 + 主翼 + 机身 + (主翼 \rightleftharpoons 鸭翼) + (鸭翼 \rightleftharpoons 机身) + (主翼 \rightleftharpoons 机身)	11 鸭翼 + 前机身 + (鸭翼 \rightleftharpoons 前机身) + (后机身 \rightarrow 前机身) + (后机身 \rightarrow 鸭翼) + (主翼 \rightarrow 鸭翼) + (主翼 \rightarrow 前机身)

* (Forebody \rightleftharpoons afterbody) indicates the summation of the aerodynamic forces generated by the interference caused by the forebody on the afterbody, and the aerodynamic forces generated by the interference on the forebody caused by the afterbody; (Afterbody \rightarrow forebody) refers only to the latter condition. The other conditions are analogous.

KEY: 1 - Model state 2 - Results of whole-aircraft balance 3 - Results of canard-wing balance 4 - Forebody + afterbody + (forebody \rightleftharpoons afterbody)* 5 - Forebody + (afterbody \rightarrow forebody) 6 - Canard wing + fuselage + (canard wing \rightleftharpoons fuselage) 7 - Canard wing + forebody + (canard wing \rightleftharpoons forebody) + (afterbody \rightarrow forebody) + (afterbody \rightarrow canard wing) 8 - Main wing + fuselage + (main wing \rightleftharpoons fuselage) 9 - Forebody + (afterbody \rightarrow forebody) + (main wing \rightarrow forebody) 10 - Canard wing + main wing + fuselage + (main wing \rightleftharpoons canard wing) + (canard wing \rightleftharpoons fuselage) + (main wing \rightleftharpoons fuselage) 11 - Canard wing + forebody + (canard wing \rightleftharpoons forebody) + (afterbody \rightarrow forebody) + (afterbody \rightarrow canard wing) + (main wing \rightarrow canard wing) + (main wing \rightarrow forebody)

From the whole-aircraft balance results, the outcome can be derived by subtracting the mutual interference between wing surfaces (that is, the main wing + fuselage + canard wing + main wing \Rightarrow fuselage + canard wing \Leftarrow fuselage)

$$C_y - \Delta C_{ywc} - \Delta C_{ycw} =$$


$$(4)$$

III. Equipment and Model

Experiments were conducted at a low-speed open 1.5m diameter wind tunnel. The angle of attack in the experiments was as high as 44° ; in the experiments, the wing speed $v=30\text{m/s}$ ($q=550.8\text{N/m}^2$). In the experiments, the Reynolds number Re was 0.52×10^6 (corresponding to the length of the aerodynamic mean chord for the main wing). The whole-aircraft balance is a hexagonal-force mechanical balance; the canard-wing balance is a strain balance. By using the oil flow method, the surface states can be observed; a fluorescing microwire mesh was used for observing spatial flow state.

The model fuselage is divided into two sections: the canard wing is on the forebody with positions adjustable as to upward, downward, forward, and rearward. The aircraft wing and the vertical tail are on the afterbody (Fig. 1). The whole-aircraft balance is connected to the afterbody. Through a rod-type strain balance (canard-wing balance), the forebody and afterbody are

connected. The parameters for the exposed canard wing and the main wing plane are the same, but the area is one-fifth of the aircraft wing area. All planes of aerodynamic forces are of the double-arc symmetric wing type.

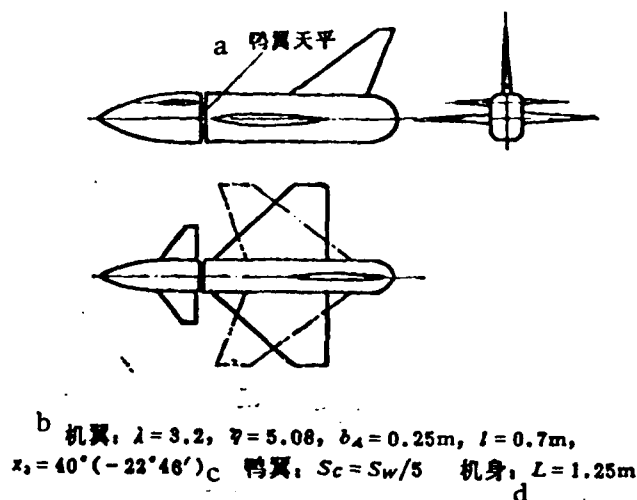


Fig. 1. Schematic diagram of model
KEY: a - Canard-wing balance b - Aircraft wing c - Canard wing d - Fuselage

IV. Characteristics of Lift Interference for Canard Configuration

1. Lift characteristics of typical situation

Fig. 2 shows the lift curves in a typical situation; the characteristic quantities are listed in Table 2. It is apparent that after installing a canard wing corresponding to 20 percent of the aircraft wing surface, $C_{y_{max}}$ can be increased by about 50 percent; the stall angle of attack α_{st} is increased by about 8° .

2. Characteristics of lift interference

Fig. 3. shows that the interference lift varies with angle of attack. When $\alpha < 20^\circ$, the summation of interference on the

main wing caused by the canard wing, and the interference on the canard wing caused by the main wing is still destructive interference. In the latter case, it is favorable to interference, but the amount is smaller. Beyond $\alpha > 20^\circ$, the superiority of close-coupled canard configuration (apparent increase in the maximum lift coefficient and the stall angle of attack) becomes evident.

TABLE 2. VALUES OF LIFT CHARACTERISTICS IN TYPICAL SITUATION

a	特征量 b	$C_L^*(\alpha = -4^\circ \sim 4^\circ)$	C_{Lmax}	α_c
	典型情况			
c	机翼-机身组合体	0.048	1.07	24°
	鸭式全机 d	0.050	1.52	32°
e	鸭式全机扣除翼面间的相互干扰	0.053	1.23	25°

KEY: a - Typical situation b - Characteristic values
 c - Aircraft wing-fuselage combination
 d - Canard-type whole aircraft e - Canard-type whole aircraft with subtraction of mutual interference between wing surfaces

3. Interference regime

From variations of the flow states on the main wing with and without the canard wing, observations were made on interferences on the main wing caused by the canard wing (Fig. 4).

In the absence of the canard wing, the flow state on the main wing is of the flow type of the typical swept-back thin wing with detached vortex. In the presence of the canard wing, generally the influence of the canard wing can be divided into

two parts: one is that the downwash of the canard wing reduces the actual angle of attack at the main wing, thus restricting the development of the detached vortex at the leading edge of the main wing within the range of small angles of attack. When the angle of attack is greater, the detached vortex at the leading edge of the main wing becomes more stable; thus the vortex lift on the main wing can be maintained to the range of even larger angles of attack. The other part of the influence is the induction caused by the detached vortex of the canard wing, thus changing the position and shape of the main wing detached vortex.

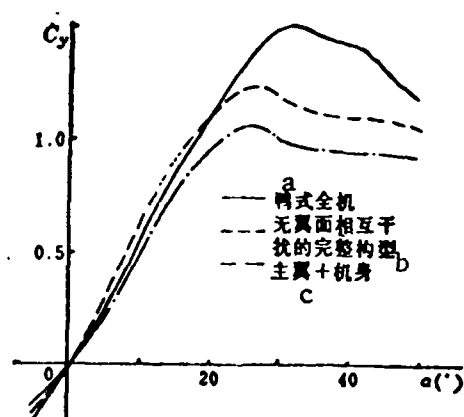


Fig. 2. Lift characteristics of typical situation
KEY: a - Canard-type whole aircraft b - Complete structural model without mutual interference between wing surfaces c - Main wing + fuselage

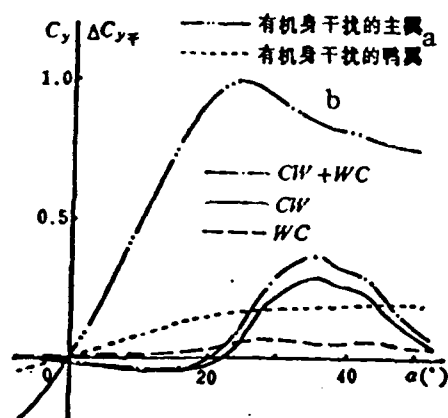


Fig. 3. Interference lift characteristics
KEY: a - Main wing with fuselage interference b - Canard wing with fuselage interference

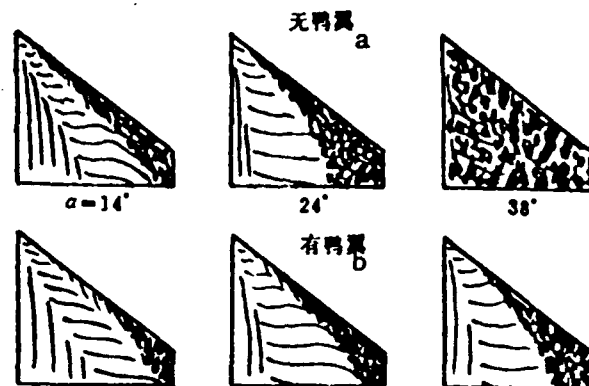


Fig. 4. Influence by canard on flow above the main wing
KEY: a - In the absence of canard wing
b - With canard wing

In the absence of the canard wing, when $\alpha = 14^\circ$, the bursting point of the main-wing detached vortex has arrived at the midsection of the aircraft wing. In the presence of the canard wing, the downwash reduces the actual angle of attack of the main wing. When $\alpha = 14^\circ$ (the actual angle of attack of the main wing is less than 14°), and then the main-wing detached vortex is weaker than the case in the absence of the canard wing, there is no vortex bursting point on the wing surface; the vortex control range is small and the vortex lift is also small. From the pressure distribution on the surface of the main wing, the canard wing downwash reduces the suction peak at the wing root of the main wing (Fig. 5), thus causing a lift reduction of the canard configuration in small range of angles of attack.

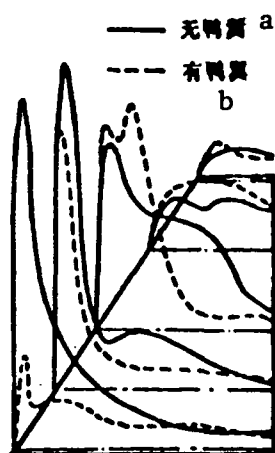


Fig. 5. Pressure distribution of main wing ($\alpha = 12^\circ$)
KEY: a - In the absence of canard wing b - In the presence of canard wing

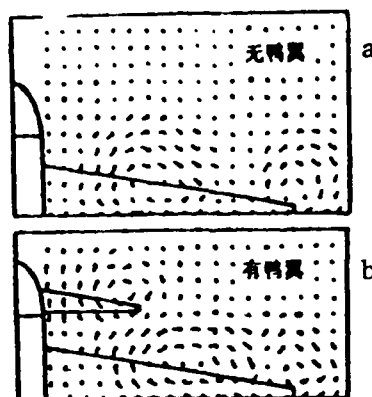


Fig. 6. Spatial flow spectrum at the trailing edge of main wing ($\alpha = 24^\circ$)
KEY: a - In the absence of canard wing b - In the presence of canard wing

When $\alpha = 24^\circ$, the bursting point of the detached vortex of the main wing in the absence of the canard wing reaches to the leading edge of the wing ring. After bursting, the vortex zone covers the upper wing surface of the main wing; in addition, a very large separation zone is induced in the zone from the leading edge to wing tip. Thereupon, the separation zone covers the maximum lift point of the main wing. In the presence of the canard wing, although the downwash of the canard wing reduces the actual angle of attack of the main wing (when $\alpha \leq \alpha_c$, the lift on the main wing is reduced), the smaller actual angle of attack of the main wing will tend to stabilize the detached vortex of the main wing, thus providing greater vortex lift. Induction on the main wing vortex by the downwash and the canard wing vortex

restricts the separation zone upstream of the vortex, and shrinks the zone. Thus, constructive interference of the canard wing is exhibited on the main wing.

Beyond $\alpha > 24^\circ$, the separation flow type of the flow direction on the main wing is developed in the absence of the canard wing. When $\alpha = 38^\circ$, there is an irregular Cauchy-Hoff separation over the entire wing surface. In the absence of the canard wing, there is a consistent regular detached vortex control zone and the reattachment zone in the wake of the vortex over the main wing surface. The induced separation zone upstream of the vortex is also smaller than that in the absence of the canard wing. Up to $\alpha = 38^\circ$, most of the wing surface is controlled by shear flow; separation is limited only to the wingtip portion. At the same angle of attack, thus, the loss of lift induced by separation over the main wing is less in the presence of the canard wing, but provides greater vortex lift. Thus, greater interference lift is generated at larger main-wing angles of attack.

Moreover, induction of the canard wing vortex not only shifts the spatial position of the main-wing vortex toward the wingtip; more importantly, the main-wing vortex has greater deformation (Fig. 6). The canard wing expands the surface area on the main wing that is covered by the main wing vortex, and expands the influence range of the low-pressure zone.

The interference on the canard wing caused by the main wing is exhibited mainly by the suction on the canard wing detached

vortex due to the low-pressure field on the surface at the main-wing leading edge (primarily, the suction peak at the leading edge), and the low-pressure field in the detached vortex of the main wing so that the interference is stronger and more stable. In this case, the canard wing also provides a constructive interference lift (at larger angles of attack, the vortex lift is larger).

4. Situation of vortex system

When the canard wing and the main wing are on the same side, they generate two detached vortices rotating in the same direction. Limited by plane parameters of two wing surfaces, the intensities of these two vortices are of corresponding values, and it is very difficult to merge into a stronger vortex over the main wing surface (it is even impossible to merge into a single vortex). Only when the sweptback angle at the canard-wing leading edge is increased to a value larger than 70° , and the height of the canard wing is basically consistent with the main wing, is it then possible. However, the total lift of this configuration is not very large, and the linearity of the longitudinal-direction moment is degraded.

V. Characteristics of Drag and Moment

At various angles of attack, all drag values of the canard configuration are slightly larger than the drag values for the conventional configuration (the canard is placed behind the main wing, thus becoming a flat tail) as shown in Fig. 7. This is because the installed canard wing lowers the suction peak at the

main-wing leading edge root, thus increasing the drag. However, at larger angles of attack, the interference lift attained for the canard configuration makes its characteristics of lift and drag superior to the corresponding regular configuration.

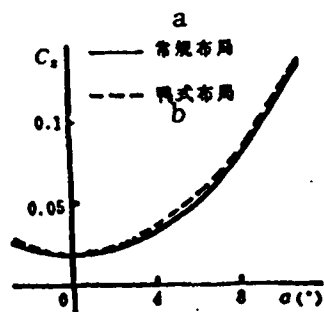


Fig. 7. Drag characteristics of canard configuration
KEY: a - Regular configuration
b - Canard configuration

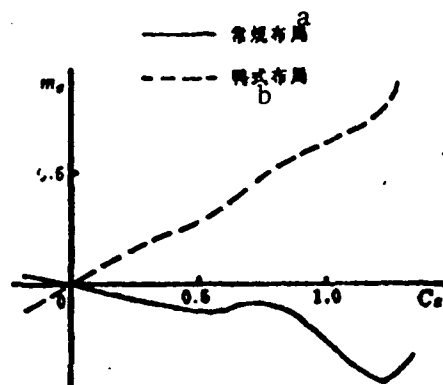


Fig. 8. Moment characteristics of canard configuration
KEY: a - Regular configuration
b - Canard configuration

For the canard configuration, the longitudinal-direction stability is of static instability (Fig. 8); however, the linearity is better in the range of very large angles of attack. This is because the flow state on the canard wing varies slowly, thus providing more stable lift; at the same time, the longitudinal-direction moment is mainly provided by the canard wing lift.

VI. Canard configuration of sweptforward wing

When the sweptback wing is changed into a sweptforward main wing (the relative position is unchanged for the aerodynamic mean chord of the two main wings relative to the fuselage; also, the

canard wing shape, size, and position remain unchanged, as shown in Fig. 1), the influence of the flow spectrum over the main wing by the canard wing is more pronounced. The separation zone at the leading edge of the root portion is apparently reduced; most of the zone over the wing surface is controlled by the local shearing flow (Fig. 9).

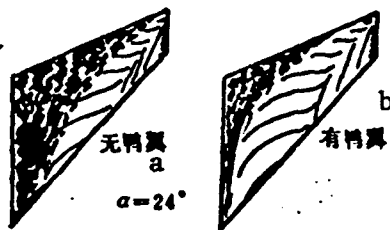


Fig. 9. Flow states over the sweptforward wing in the presence, and in the absence of the canard wing
KEY: a - In the absence of the canard wing b - In the presence of the canard wing

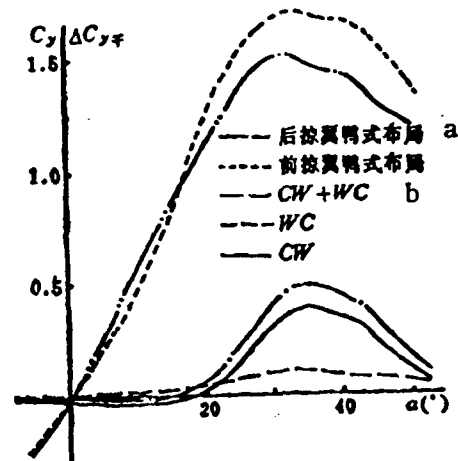


Fig. 10. Lift characteristics of sweptforward main wing in the canard configuration
KEY: a - Sweptback wing canard configuration b - Sweptforward wing canard configuration

In the sweptforward main wing of canard configuration, better lift characteristics are exhibited at the median angle of attack [1]. When compared with the sweptforward main wing, canard configuration, the maximum lift coefficient is increased by 0.2; there is an apparent nonlinear lift, but the stall angle of attack is the same (Fig. 10).

This research received guidance from professor Luo Shijun, as well as colleagues Qin Peizhao and Fan Jiechuan. Colleagues

Wang Xuejian and Zhang Binjiang took part in the experimental study. The author expresses his gratitude.

The first draft of the paper was received on 15 September, 1989; the final revised draft was received for publication on 6 March 1990.

REFERENCES

1. Zhang Lizhuang, Wang Xuejian, Guo Yaobin, and Zhang Binjiang, "Low-speed aerodynamic study of sweptforward wing," in: Zhanguo Hangkong Kexue Jishu Wenxian [Papers on Aerodynamic Science and Technology in China], HJB830108, 1983.

DISTRIBUTION LIST

DISTRIBUTION DIRECT TO RECIPIENT

<u>ORGANIZATION</u>	<u>MICROFICHE</u>
B085 DIA/RIS-2FI	1
C509 BALLOC509 BALLISTIC RES LAB	1
C510 R&T LABS/AVEADCOM	1
C513 ARRADCOM	1
C535 AVRADCOM/TSARCOM	1
C539 TRASANA	1
Q592 FSTC	4
Q619 MSIC REDSTONE	1
Q008 NTIC	1
Q043 AFMIC-IS	1
E051 HQ USAF/INET	1
E404 AEDC/DOF	1
E408 AFWL	1
E410 ASDTC/IN	1
E411 ASD/FTD/TTIA	1
E429 SD/IND	1
P005 DOE/ISA/DDI	1
P050 CIA/OCR/ADD/SD	2
1051 AFIT/LDE	1
P090 NSA/CDB	1
2206 FSL	1

Microfiche Nbr: FTD93C000463
FTD-ID(RS)T-0730-92